Stress Corrosion Cracking Rates for 7079-T6 Sheet

Molly R. Walters, Sandeep R. Shah and Scott A. Fawaz
Center for Aircraft Structural Life Extension (CAStLE)
Department of Engineering Mechanics
United States Air Force Academy
Colorado Springs, Colorado 80840

Abstract

Stress corrosion cracking (SCC) is a well known problem in AA7079-T6. In a large transport aircraft, efforts are underway to replace the fuselage skin made of this alloy to counter the SCC problem. Some of the replaced panels were analyzed to study the root cause of failure. Most of these cracks initiated at the forward and aft edges of the panel, where there is no clad layer. Nucleation of these cracks was undoubtedly from corrosion pits. The cracks propagated inward from the free edge of the panel in the LS direction and deviated to the LT orientation along mid-thickness. All the macro features suggest that the crack has propagated by SCC. Detailed mechanical and metallurgical analysis of the skin panel suggests that the cracks in the LS orientation propagate due to SCC and the mid-thickness LT crack propagates by fatigue.

To understand the crack growth kinetics in detail, experiments were performed to find SCC crack growth kinetics. The SCC crack growth rates were determined in K-increasing and in constant-K tests. In increasing-K tests, both constant load and constant displacement modes were used in three different environments: a) de-ionized water fog, b) 3.5 mol/L NaCl solution bath, and c) saturated NaCl solution bath. Two test frames were fabricated in-house for constant displacement tests. Mechanically driven universal test frames were used to conduct experiments in constant load modes using a computerized feedback system to control displacement and to maintain constant load. These tests yielded higher threshold K_{ISCC} values for every test when compared to the OEM report, regardless of environment or loading type. Crack growth rates were consistently lower for specimens tested in de-ionized water and higher than the published value for 3.5 mol/L NaCl and saturated NaCl solution bath. Little difference was noted between the specimens tested in the 3.5 mol/L NaCl condition and saturated salt condition.

Constant K experiments were conducted in saturated salt solution bath only to get extreme growth rates. LabVIEW in conjunction with a computer-controlled servo-hydraulic test frame was used for real-time crack length and K calculations and load was adjusted to maintain constant K. Constant K experiments were done in static mode as well as some superimposed fatigue loading also. Fatigue superposition was only ±2 ksi√in over mean constant K. The crack growth rate was very similar for both static and fatigue SCC test. This suggests that if SCC is a dominant crack growth mechanism, superimposed fatigue does not affect the crack growth rates at frequencies up to 10 Hz. If cracks do propagate by fatigue at low frequencies, SCC does not have any contribution on crack growth rate. However, corrosive environment may affect the fracture energy values.

I. Introduction

The aft crown skin of a large transport aircraft is extremely susceptible to stress-corrosion cracking (SCC) due to combination of three essential parameters: presence of tensile stresses, corrosion susceptible material, and corrosive environment in service. SCC has become a major problem on this aircraft, especially since this aircraft is made with legacy 7079-T6, where SCC is a known problem. In recent past large cracks were found on in-service aircrafts which were more than double the size of allowable crack size in that area. These cracks were attributed to SCC and since there no definitive models for predicting SCC crack growth most of these aircrafts undergo inspections at very short regular intervals increasing the inspection/maintenance burden on the depot. In order to properly maintain the aircraft, high confidence SCC crack growth rates must be determined to shift the "find and fix" approach at depot to "anticipate and manage."

SCC crack growth rates are well characterized for thick materials, forgings and extrusions, but for thin sheet material the data is almost non-existent. The original equipment manufacturer (OEM) has used data from an old contractor's report (Figure 1). Data in the report is from unknown sources from and

specimen type, loading method and environment type are not mentioned. This is one of very few sources from which the OEM may predict SCC crack growth rates for 7079-T6. As seen in Figure 1, the threshold for SCC, K_{ISCC}, is 6 ksi√in in the transverse direction and 10 ksi√in in the longitudinal direction. The purpose of the present study is to confirm these values, along with the nature of the plot. In the OEM data, region II of SCC crack growth shows a steady increase in crack growth rate. Most of the published SCC data for variety of aluminum alloys show a steady crack growth rate in region II.   It is therefore necessary to obtain data under controlled experimental conditions and verify the nature of the crack growth curve.
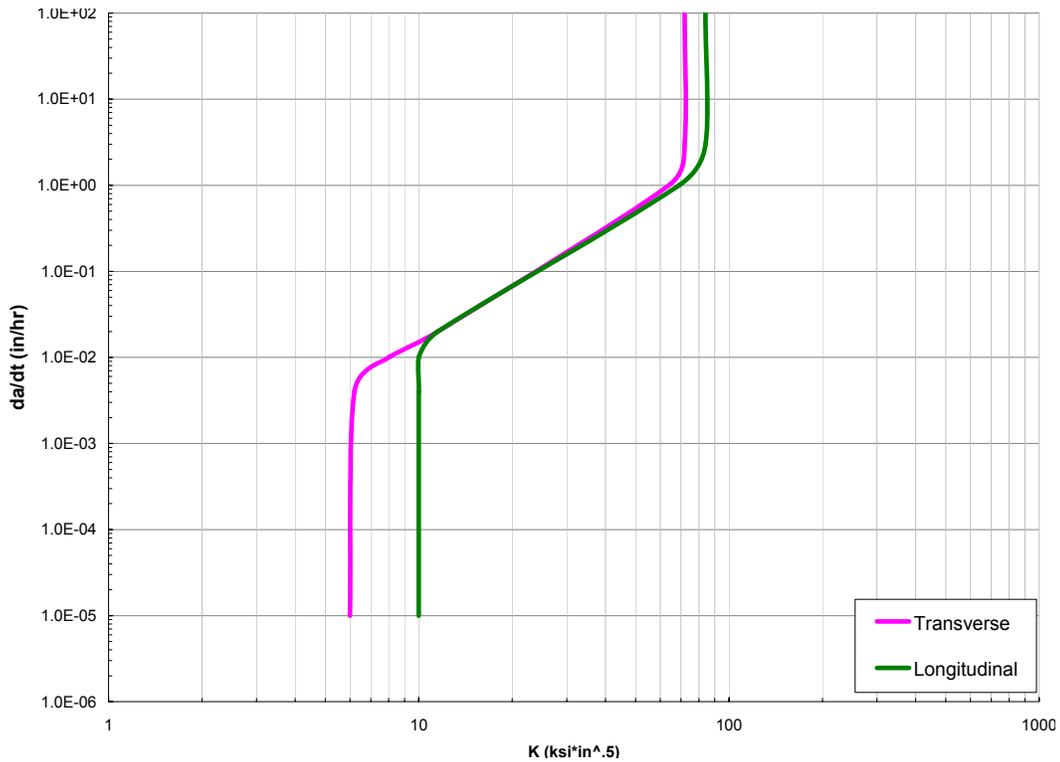

Figure 1. The OEM is currently using this unsourced data for their crack growth rate prediction models. The K_{ISCC} values for this data are 6 and 10 ksi√in for the transverse and longitudinal directions, respectively.

II. Background

At the center for aircraft structural life extension (CAStLE), we had received some AA7079-T6 crown skin panels, removed from one such large transport aircraft. Detailed investigation of the panel revealed extensive cracking at the forward and the aft edges of this panel. Figure 2 shows a typical cross sectional micrograph of one such crack.

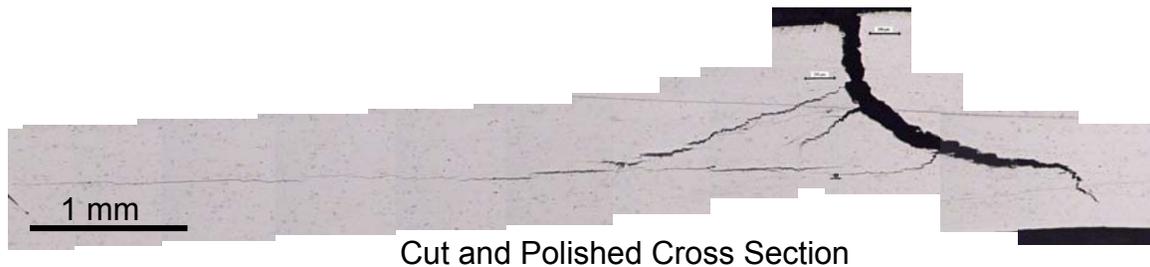

Cut and Polished Cross Section

Figure 2: Cross section micrograph of a typical crack on crown skin panel showing extensive branching and propagation of sub-surface in-plane cracks.

2

The crack shown in figure 2 initiated at the forward edge of the panel, just below the clad layer from extensive pitting. While propagating in aft direction from the initiation site, the crack branched and propagated in in-plane orientation just beneath the surface. This kind of crack growth is even more alarming as there are no suitable NDI techniques to confidently verify in-plane crack in a typical layered structure with sealants and paint between the layers. When these cracks were opened and analyzed in detail, significant corrosion deposits were noted on the surface of the crack. Washing of these products revealed the presence of striations on the crack surface as shown in figure 3.
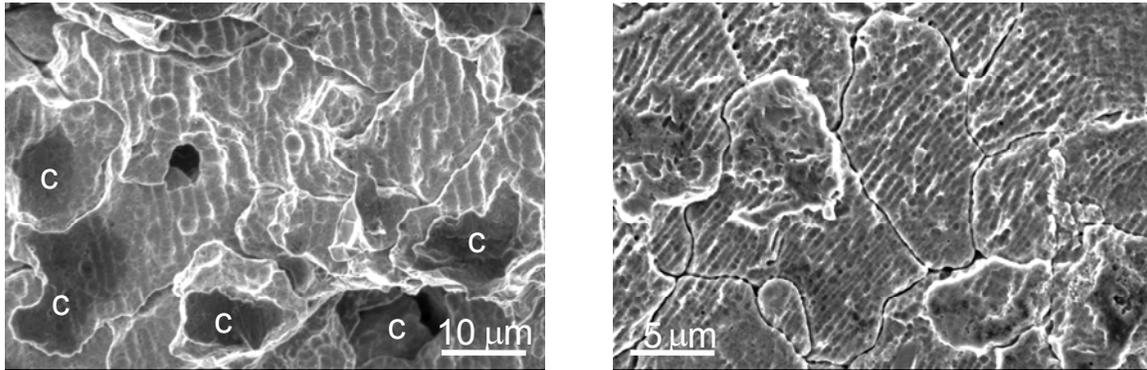

Figure 3: Crack surface after removal of corrosion products, showing striations on the surface.

This observation leads to intriguing questions about the crack growth mode in this panel. It is quite likely that SCC and fatigue both crack opening mechanisms are both operating. To separate out the effect of two mechanisms, it is necessary to know definitive crack growth rates in two mechanisms separately and combined together. In the present study we focus on getting reliable SCC growth rate data.

SCC is commonly dependent on the stress intensity at the crack tip. Stress-corrosion crack propagation takes place only when the stress intensity is above a threshold value. The threshold stress intensity determination was not done as part of this test program since it would take an extreme amount of time to determine accurately. Hertzberg[2] has noted that for aluminum alloys, to determine the threshold stress intensity, minimum test duration should be about 10,000 hours (over 416 days). In this particular scenario, the material used was high strength aluminum alloy 7079-T6, prone to corrosion and SCC in the presence of corrosive environment and stress. 7XXX Series alloys are notorious for SCC problems, especially those in the –T6 temper, the peak-aged, condition due to the presence of alloying elements such as zinc and magnesium which can act as a cathode, and copper, which acts as an anode, leading to galvanic corrosion in presence of an electrolyte. In this case of SCC, the acting electrolyte is humid air, often found at the aircraft's basing locations.

Speidel[3] has shown in SCC tests of thick sections such as die forgings and plates of 7XXX alloys that 7079 has much higher crack growth rates in Region II, about 1000 times higher, than 7075, see figure 4(a). Figure 4(b) shows the effect of concentration of halide ions on SCC crack growth of AA7079. This plot suggests that the effect of concentration is more dramatic at lower levels of concentrations; however the difference in the crack growth rate above 5 mol/L halide salt solution concentration is very marginal. In this study, the experiments were conducted in a de-ionized (DI) water fog (a mild environment), 3.5mol/L NaCl solution bath (typically comparable to an in-service corrosion environment, and a standard for corrosion tests) and saturated, or 6.15 mol/L, NaCl solution bath to study the extreme case scenario. Temperature was not monitored since all tests were done at the ambient temperature.

The specimens for this study were taken from a panel of the original fuselage crown skin which was replaced after noticing cracks. Care was taken to avoid any defects in the specimen while cutting them from the panel. For the first set of tests, the primer and paint were kept almost intact except at the notch. The paint was removed near the notch area to allow for an electrical path during electrical discharge machining (EDM) of notch. However, in the later tests, coatings and primers were completely removed. Surprisingly, the specimens with coatings and primers removed exhibited almost two decades slower crack growth rate as compared to their un-stripped counter parts. The in-service panels are coated with chromate
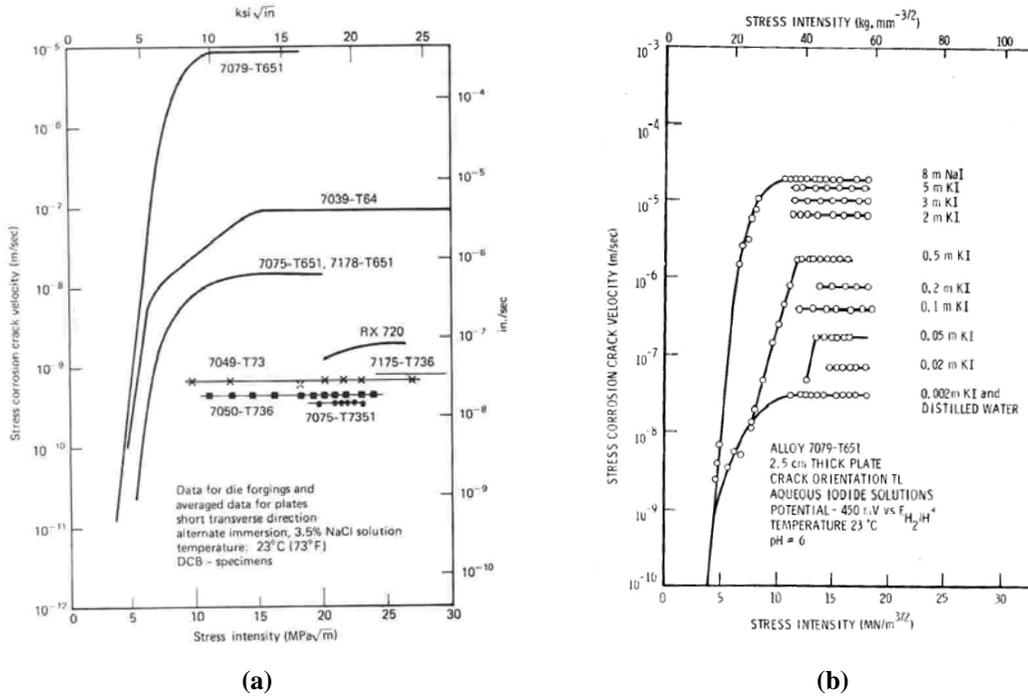
(a)   (b)

Figure 4 (a) Speidel[3] has done SCC tests in a 3.5% NaCl alternate immersion environment, showing very fast crack growth rates for AA7079. These tests were done on thick material, 2.5 cm, which often yield slower crack growth rates than thin sections of the same alloy. (b) Effect of halide salt concentration on the SCC crack growth rate of AA7079-T651 thick plate. This plot shows the dramatic effect of lower concentration on crack growth as compared to higher concentrations and 8 mol NaI solution shows comparable growth rate to 2-5 mol solutions (after Speidel[3]).
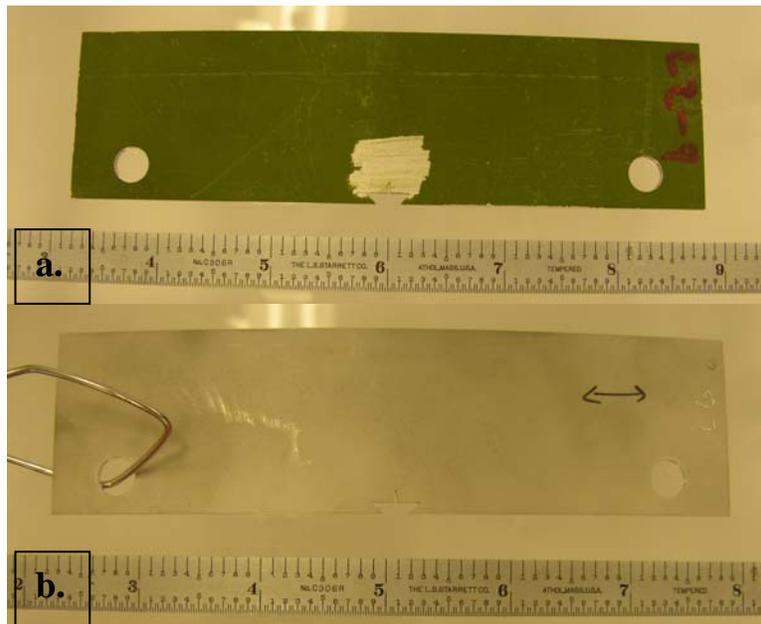

Figure 5. Coated and uncoated samples. Figure "a," above, has chromate coating covering the surface except for the machined edges of the part and the notched portion of the sample, where coating removal was necessary to machine the notch with EDM. Figure "b" was soaked in acetone to soften the coating, then scraped clean before final machining.

4

conversion coatings, widely used in 1960s and 1970s. The accelerated crack growth rate in specimens with coatings could be attributed to preferential corrosion in the uncoated area. Simply, on an uncoated sample, corrosion may attack at any surface since there is no chemical or physical barrier to prevent it, it may propagate evenly. On a coated sample, the edges and the machined notch are the only exposed areas of the sample where corrosion may occur until there is a crack, see Figure 5. Then the crack will be more likely to suffer preferential corrosion because fresh material is constantly being exposed as the crack propagates.

Since the mode of loading is not well understood on the crown skin, experiments were conducted in constant displacement, constant load and constant K configurations. Constant displacement depicted the actual structure where the components shed load as the crack propagates, since the structure is fixed, whereas constant load depicts an extreme loading condition, such that the stress intensity factor increases monotonically with crack growth. However, since the data was collected as a function of the stress intensity factor, the two methods resulted in different growth rates only based on environmental exposure time, which would be longer in the case of constant displacement. Constant K experiments were done to confirm the crack growth rates for a given stress intensity.

III. Experimental Methods

For this program, the specimens were machined from an actual aircraft skin since this is the only material available. Incidentally, 7079-T6 has not been commercially available for many years. Testing the actual aircraft skin does have other benefits. The sheet manufacturing process, age degradation, and environmental exposure is nominally the same for the skin tested and the remaining skins on aircraft.

Since the skin is thin, less than 0.08", the only geometry that could be used per ASTM Standard E 647[4] is an ESE(T), an eccentrically-loaded single edge crack tension specimen, see Figure . As compared to the popular C(T) and M(T) specimens for SCC tests, the ESE(T) was desirable because the material is thin and has a relatively long test section. Length of the specimen was a critical dimension in these tests since the specimen had to be placed in an environmental chamber. Also, ESE(T) has compliance equations available in the standard, which can be easily used to monitor the crack growth without periodic interruption of the test to measure crack length.
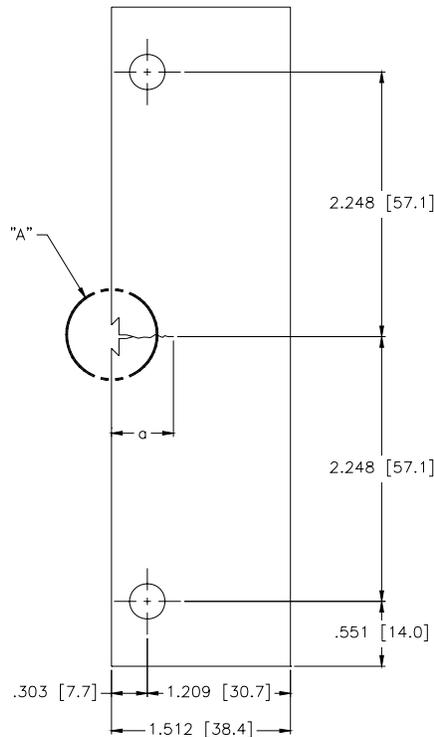

Figure 6. ESE(T) specimen per ASTM E 647. The dimensions are shown in English units with metric units in brackets.

Use of the compliance equations was verified by fractography. In this case an ESE(T) specimen was instrumented with a COD gage and a back face strain gage was used. The specimen was cracked in fatigue using a marker spectrum. At the end of each set of marker bands, the specimen was loaded to a predetermined load and COD and strain gage readings were taken. These readings were converted to equivalent crack length using the compliance equations provided in the standard. The failed specimen was then observed in a SEM to identify the end of each marker band cycle and to measure its distance from the edge of the specimen. The crack lengths at the end of each set of marker bands were then compared with the distance of the marker band from the edge. The crack length determined from the COD gage reading and strain gage reading compared well with those observed in the microscope.

Specimens were machined using a computerized numerically controlled (CNC) milling machine and an electrical discharge machine (EDM). After machining, the specimens were pre-cracked using hydraulic MTS test frames as described in the aforementioned ASTM Standard. A maximum load of 220 lbs (2.2 ksi) was chosen for pre-cracking to keep K under 5.5 ksi√in. Instrumentation used for pre-cracking was a 5mm crack opening displacement (COD) gage and back face strain gage. Using the compliance equations in the ASTM Standard, the approximate COD value for a 0.295" crack was 0.00102" for a 0.0675" thick specimen and strain gage value was -350 microstrains. The fatigue frames were set to run 150,000 cycles or to when the COD limit was exceeded. Specimens usually ran about 100,000 cycles to create a crack about 0.295" in length from an EDM notch of 0.185". The programmed mean load was 120 lbs (1.2 ksi), the amplitude was 100 lbs (1.0 ksi), and frequency used was about 20 Hz. The frequency used varied by the test frame used.

A. Instrumentation

Since the specimen was to be inserted in an environmental chamber for testing, crack growth via optical readings would be very difficult. Compliance is an accepted method of tracking crack growth rates for ESE(T) specimens. During preliminary testing, it was found that front-face compliance with a COD gage was difficult to use in the chamber and a small amount of misalignment of the COD gage resulted in erroneous results. Also, the thin nature of the specimen allowed little to no self-alignment capabilities of the COD gage, leading to errors. In addition, strain gages are more resilient than COD gages in harsh environments if the proper adhesives and coatings are used. So the back face strain gage compliance was used reliably in the present investigation. The equation for fitting a fourth-order polynomial containing back-face and front-face compliance was given in the ASTM Standard.

The strain gage had to be very narrow so that it could fit on the thickness edge of the crown skin material. TML strain gages (type FLK-1-23) were used for this purpose. The gage width was 0.028" and the width of the backing was 0.055". Each gage was carefully applied so the gage was centered in the thickness of the specimen and the EDM notch was directly in line with the gage lengthwise. Finally, to protect the gage from humidity, beeswax was applied once it was bonded. The use of beeswax coating is well-known in corrosion studies, therefore it was used here. Later, for ease of use, silicone was substituted.

B. Test Apparatus

Initially, constant displacement tests were considered the best option because they would provide slow cracking and near-constant K values. This would be beneficial because data was to be taken manually. For this type of test, a frame, see Figure 7, was built from 2" square steel tube and the final assembly consisted of a load cell, Lebow 1000 kg capacity, connected to a clevis. The specimen was linked to another clevis on top. Chain was connected from the specimen's top clevis to a yoke with a threaded rod attached to the frame. The rod went through the top of the steel tube and came through the top of the frame. There a washer and nut secured the threaded rod such that the specimen was maintained at a constant displacement.

Collecting data through the three stages of SCC growth was desired; however, the constant displacement test started at a lower K value would take a very long time to propagate to the third region of crack growth. Alternatively, with constant load testing, SCC cracking would progress more quickly and the equipment could be easily configured to take data automatically. Thus, constant load tests were also performed on mechanically driven universal test frames from SATEC and constant K tests were performed on servo-hydraulic MTS frames. In the end, data was collected via all three test procedures.

6

Figure 7. Constant displacement load frame with DI water fog environment.

Figure 8. Specimen tested with cup in place for bath. Strain gage wire is also visible. No grips are immersed in the bath.

C. Introduction of Environmental Effects

Two types of environmental chambers were used. In one setup the environment was introduced by enclosing the specimen in a clear chamber. One end of the cylindrical tube was fixed and the other side had a door that could be slid off easily to insert the COD gage, if required. To introduce humidity into the chamber, a lab air supply was connected to an Erlenmeyer flask containing the solution for the particular test on top of a hot plate. In the flask, an air stone was attached to the tube with the incoming forced air. The heat from the hot plate and the agitation from the air bubbles created air with saturated humidity, which was passed into the test chamber. Humidity levels were verified visually. Humidity was considered acceptable if condensation was present on the chamber wall.

Another chamber was used to present a more severe condition at the crack tip. The environmental bath was created by cutting a small slot in the bottom of a plastic cup, then sealing the cup to the specimen with RTV silicone manufactured by Accumetric, Inc., see Figure . The solution could be poured into the cup and levels could be maintained to keep the crack submerged.

There were three environmental conditions for this test. The first one was deionized water fog using a test chamber as shown in Figure 7. This was tested to provide the most conservative bound of crack growth rates. Second, a saturated salt solution using the solution bath as shown in Figure . This was created by stirring NaCl, non-iodized table salt, into deionized water until no more of the salt could be dissolved. Last, a 3.5 mol/L NaCl test; it was prepared by adding 204.55g of table salt to 1L of deionized water again using the solution bath as shown in Figure . The saturated environment was tested as it was expected to accelerate crack growth to a maximum value as per the plot in **Error! Reference source not found.**.

A saturated calomel electrode (SCE) was submerged in the saturated salt solution to monitor corrosion potential. The electrode used was manufactured by Accumet; The electrode potential was recorded during the duration of crack and no significant change was seen during the test duration.

D. Test Set-Up

Constant Displacement

First, the specimen was inserted into the test chamber and attached to the test frame by affixing the clevises to the top and bottom of the specimen. The chains and clevises were aligned so torque would not affect the specimen. The nut was tightened so that desired tension was applied to the specimen. As the nut was tightened, the load cell would give load readings once per second. The nut was tightened slowly until the load cell's value was the desired initial load. Time, load, and strain data were recorded once every minute using the LabVIEW data acquisition software. Even though the constant displacement type test was more time consuming and did not always produce a full curve of results, it was still useful because the material could have performed differently as it has been exposed to a harsh environment for a long period of time.

Constant Load

The specimen was first inserted into the environmental chamber and then pinned into the clevises. An automated test program was created within Partner v.6.0b from Instron/SATEC Systems to apply a given load, and maintain it constantly throughout the duration of the test and collect data. Similarly MTS hydraulic frames with Teststar IIm software were also used. Time, displacement, load, and strain were recorded each minute.

Constant K with LabVIEW

After preliminary analysis, it was recognized that constant displacement tests did not provide truly constant K testing. In order to have constant K tests, a controller was required with continuous active feedback in order to calculate current crack length and required load to maintain K. Ready-made test software with this capability is not available in the lab, so LabVIEW was incorporated to perform this function. For each test, input values were specimen dimensions and the desired K value. Active feedback would be sent to the computer-controlled, servo-hydraulic test frames in order to deliver the required load. Data acquisition was done with MTS Teststar IIm. This LabVIEW method was used to incorporate a static SCC test at a constant K and fatigue SCC test with constant K_{mean} and ΔK of ± 2 ksi√in at frequencies of

0.01, 0.1, 0.5, 1 and 10 Hz. This was incorporated to study the effect of small cyclic loading on SCC growth rates.

Analysis

As mentioned before, strain data was converted to crack length via compliance equations in ASTM E 647. Continuously monitored strain gage data was then converted to crack length and plotted as a function of time. The crack growth rate was determined from the first derivative of the crack length vs. time data. After a suitable curve was fit to the crack length versus time curve, the derivative of curve fit equation was used to calculate da/dt and plotted against K, which was also calculated based on equations provided in ASTM E-647. The test data was then compared to data shown in figure 1.

IV. Results

The crack growth rate versus stress intensity plots for the different environments are shown in figures 9, 10 and 11.. Also noted are the initial loads and initial stress intensity values for each test. In the results for the deionized water fog, Figure 9 shows rates about one decade lower than the OEM data and the K_I, initial stress intensity, values are higher than the transverse direction data—about 10 ksi√in rather than 6 ksi√in.
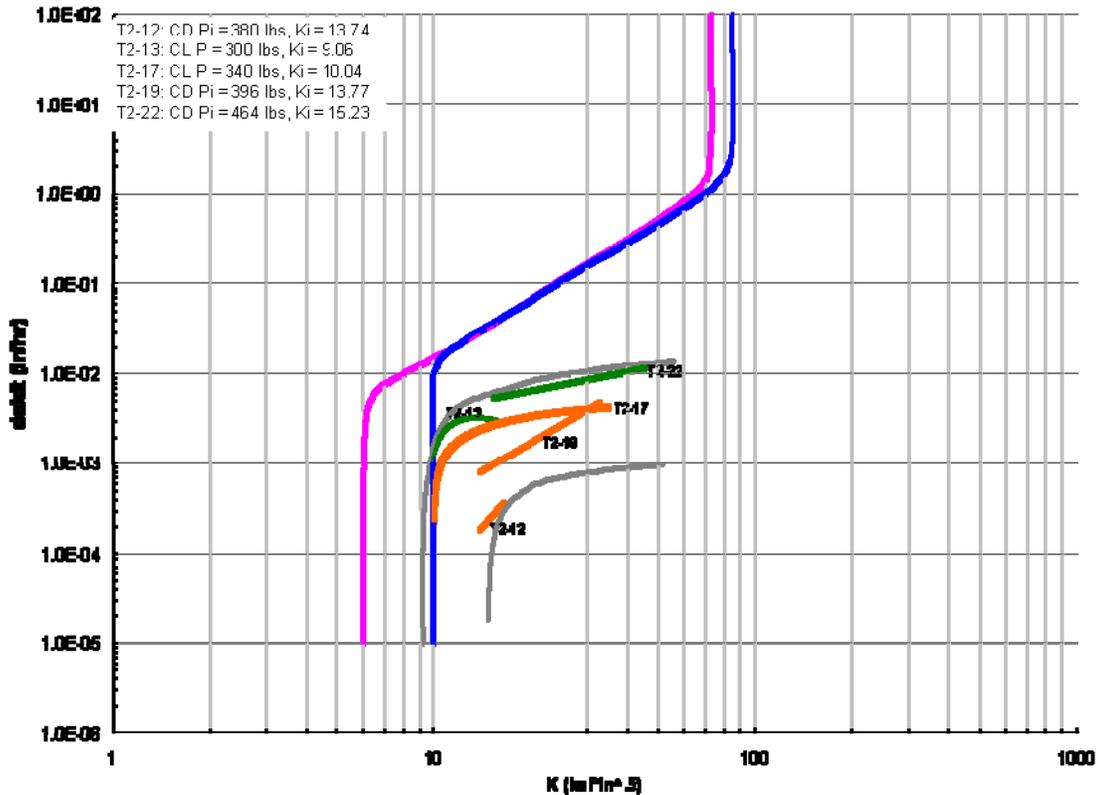

Figure 9. Crack growth rate versus stress intensity for deionized water fog. Scatter bands have been drawn in gray. In the legend, constant displacement is denoted by CD and constant load is CL. Rate data is much lower for this environmental condition, while K_I values are consistently lower than the published transverse data—about 10 ksi√in rather than 6 ksi√in.

The crack growth rates for 3.5 mol/L NaCl bath were all higher than the OEM data. Initial stress intensity values were all lower than the test data in the DI fog condition, yet they were all higher than the referenced data. Three specimens were tested in this condition, see Figure 5.
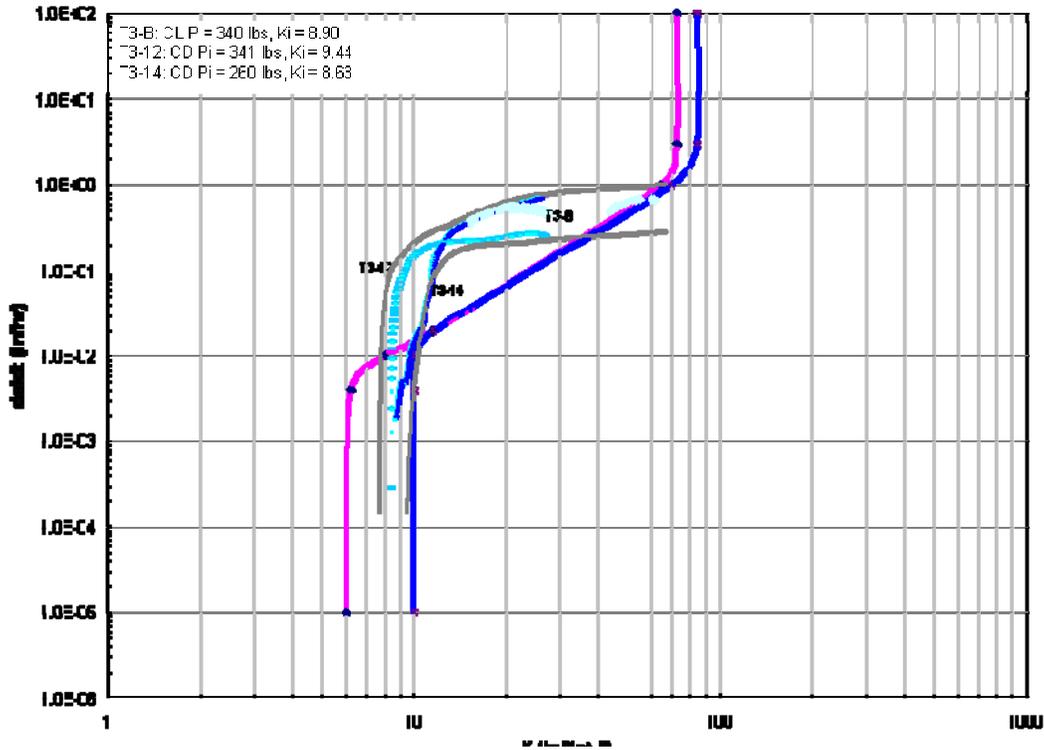
Figure 5. Crack growth rate versus stress intensity in a 3.5 mol/L NaCl Bath. Scatter bands have been drawn in gray. In the legend, constant displacement is denoted by CD and constant load is CL.
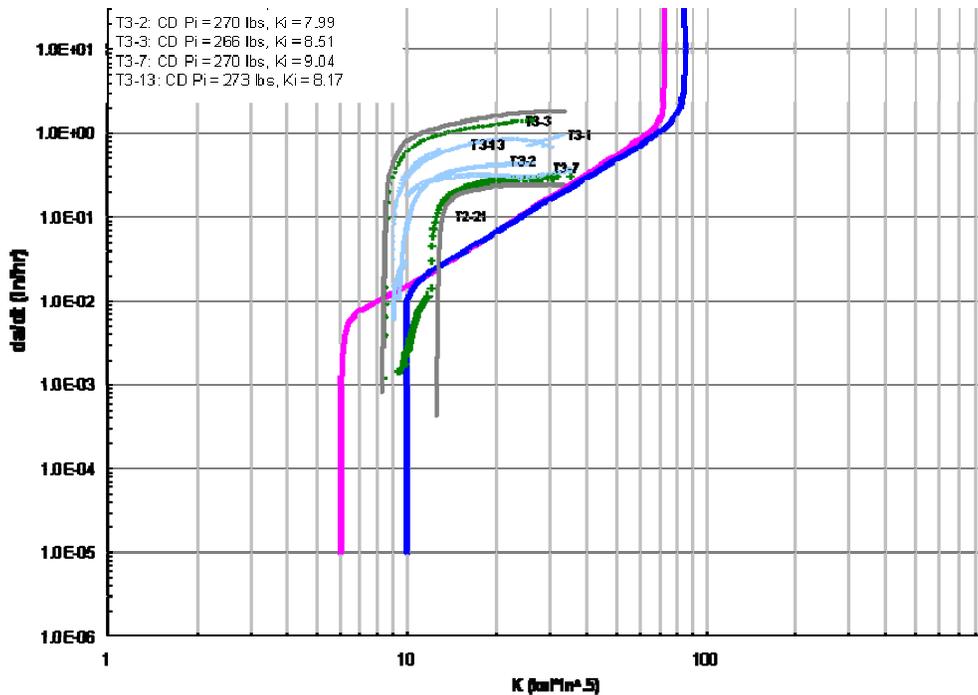

Figure 6. Crack growth rate versus stress intensity for saturated salt bath. Scatter bands have been drawn in gray. In the legend, constant displacement is denoted by CD and constant load is CL. Scatter is greater in this data set; about one decade wide, but this data set also presents the fastest growth rate found during this program—over one inch per hour.

The set of specimens tested in the saturated salt bath had one specimen with particularly high growth rate, over 1.00 inches per hour, see specimen T3-3 in Figure 6. Also, this set of specimens yielded the lowest calculated K_{ISCC} value; specimen T3-2 initiated a crack at 7.99 ksi√in. Saturated salt and 3.5 mol/L NaCl baths had very similar crack growth rates. The aggressive environments showed much higher crack growth rates than the DI water fog. For all three environment types, most specimens had relatively flat crack growth regions, whereas the OEM data did not show a region of constant crack growth rate.

All these experiments were carried out on partially stripped specimens with coating intact on most part of specimen except near the notch. Constant K experiments were carried out on completely stripped specimens. Accelerated crack growth rate was observed for coated samples when compared to uncoated samples. See Figure 7. Corrosion potential was monitored for the later tests, submerged in saturated salt solution. See Figure 8. Figure 15 is a master plot of all the data showing constant load and constant displacement plots for coated specimens in comparison with constant K plots of coated and uncoated specimens. It also includes the data of constant K tests with superimposed small fatigue of ± 2 ksi√in over constant K_{mean}.
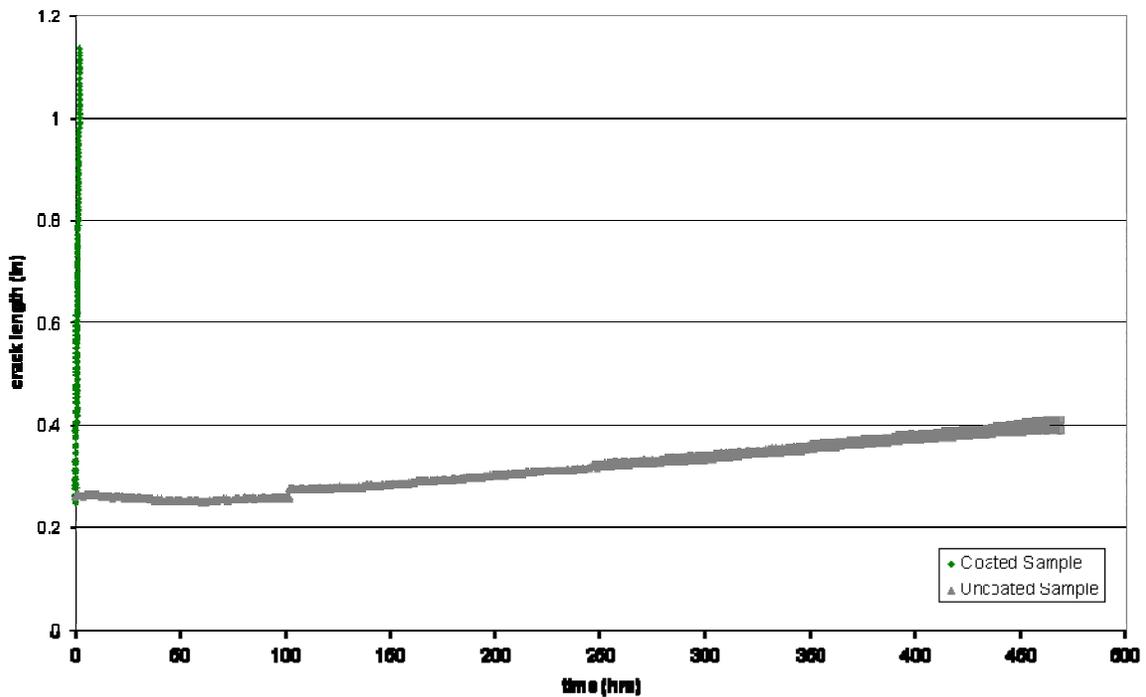

Figure 7. Crack velocity for coated and an uncoated specimen, both tested at 20 ksi√in. These samples were tested in a saturated salt bath.
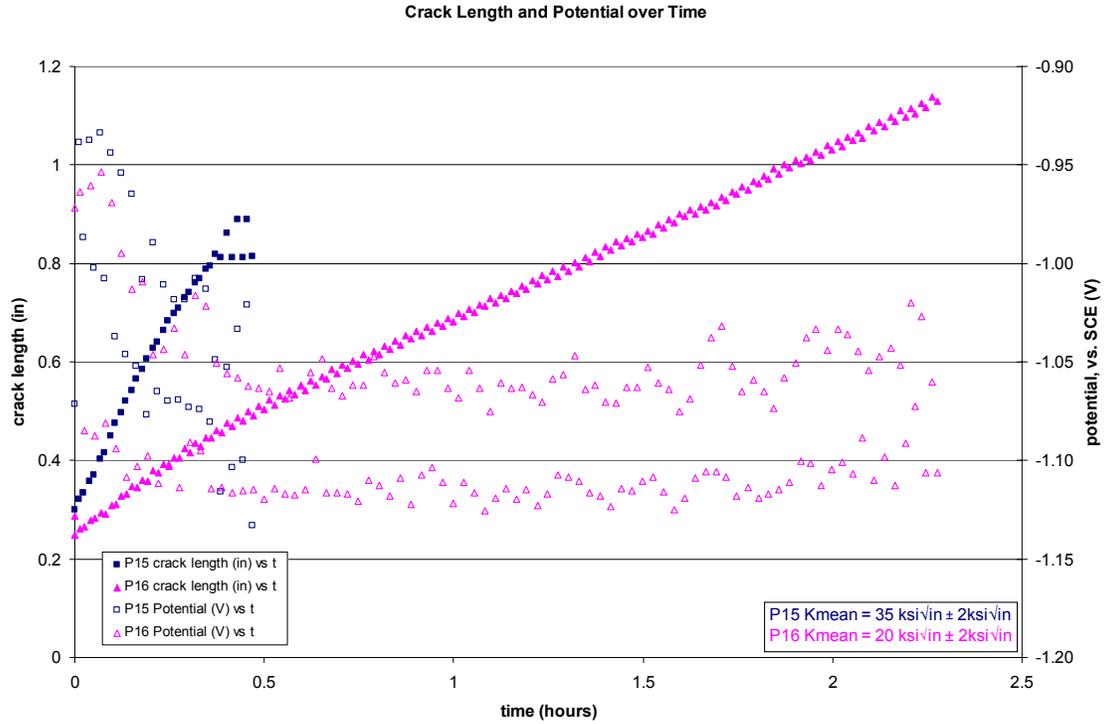
Crack Length and Potential over Time

Figure 8. Crack growth rates and potential versus time for two coated samples with different stress intensity values.
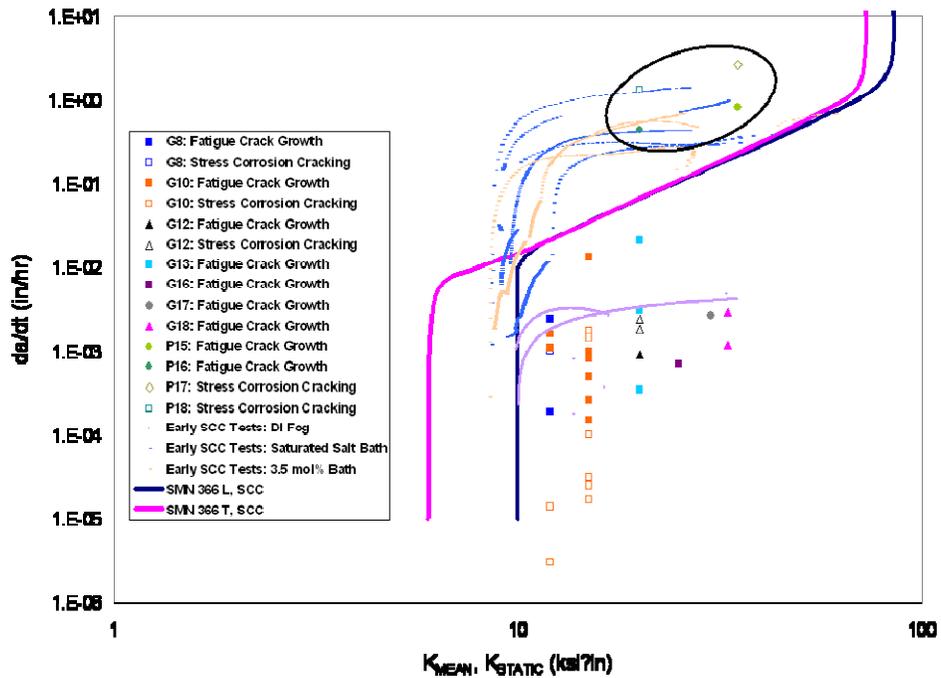

Figure 9. All tests were done in saturated salt solution. Crack growth rates were highest for coated samples. That data is circled. More detailed tabular data can be found in Appendix E.

12

As mentioned earlier, LabVIEW was incorporated into the test plan so that fatigue and SCC crack growth rates could be studied together with constant K_{mean}. This was the closest method to determine if fatigue during the SCC crack growth would have any significant effect on crack growth rate. Some pure fatigue crack growth experiments were planned if there was a substantial difference to accurately separate out the effect of each crack growth mechanism. However, as shown in Figure 9 there was no difference in crack growth rate for static or fatigue SCC. It can therefore be concluded that SCC growth rate is much faster than fatigue for frequencies below 10 Hz.

V. Discussion

The material provided to CAStLE was curved in the longitudinal direction of the specimens, the transverse direction of the material. Since this material was taken from the skin of the aircraft, the curvature was inevitable. However, in failure analysis, the fracture surface did not reveal any characteristics that would suggest a bending stress affected damage propagation or final failure. The very large radius of the structure helped to lend confidence that little effect would be found from bending during this test program.

All specimens were tested in the short transverse direction. When compared to the curves in OEM data, initial stress intensity values were about 25% higher in this test program. K_{ISCC} values in OEM data were about 6.0 ksi√in. Since this study yielded much higher initial stress intensity values than the referenced data, a threshold test was initiated. A specimen placed in a saturated salt bath loaded in constant displacement mode has been tested for over 400 days with very little change in load—about ten pounds, maybe due to drift in the load cell's inherent design suggesting no crack growth. The initial K value chosen for this test was approximately 7.1 ksi√in. The test will be monitored for next few months to see if the threshold is really lower than 8 ksi√in.

Data for the fast fracture portion of the test could not be captured reliably. For ESE(T), only 80% of the width may be cracked for the compliance equations to be valid. Most specimens were tested to the maximum crack length, but no region III type of a curve was observed. The differences in initial load values did not change crack growth rates. No correlation, however, was found between initial load and crack growth rates.

There was little difference between the results from the 3.5 mol/L NaCl and the saturated salt solution. It was uncertain when the test began if more severe crack growth rates would be result when using a saturated solution rather than the 3.5 mol/L solution. From the results presented, it seems there is marginally higher crack growth rate in the saturated condition.

There was no difference seen in the crack growth rate for constant K tests with static loading and superimposed fatigue loading at frequencies from 0.01-10 Hz. This suggests that the static SCC growth rate is more dominant as compared to fatigue crack growth rate in AA7079-T6 material, for frequencies less than 10 Hz.

Specimens containing intact coatings experienced higher crack growth rates than those with no coatings. The reason for this is not clear. The primer and paint stop any electrochemical reaction from occurring on the surface of the specimen. The reaction may be localized where the AA7079 directly interfaces with the salt solution. This may lead to preferential attack and accelerated crack growth.

VI. Conclusion and Recommendations

All the three methods of testing, namely, constant load, constant displacement and constant K, provided similar crack growth rate data for a given K. The loading rate or duration of test did not have any significant influence on the crack growth rate.

The present study shows that SCC growth rates provided in OEM data are averaged between the growth rates measured in the deionized water fog environment and the saturated salt bath immersion environment. The difference between the two sets of data is over 3 orders of magnitude. The other major finding in this study is that K_{ISCC} is comparatively higher than that suggested in OEM data. Current experiments in our laboratory suggests that minimum K_{ISCC} is about 8 ksi√in.

Test data showed slopes in steady state crack growth regions were nearly flat, whereas in OEM data, the crack growth rate slightly increased as stress intensity increased. This could be due to a change in the mode of loading or the specimen type. However, the literature normally shows a flat plateau region rather than continuously increasing crack growth rate with stress intensity factor.

The other significant finding of this study is that the crack growth rates are much lower, about 2 orders of magnitude, when the primers and coatings from the specimens are completely stripped away. The data from OEM compares well with the specimens with coating and primer, so the maintenance intervals may not be significantly affected by this finding. However, a detailed study is required to understand the effect of coating and primer on SCC growth rates.

The combined effect of fatigue and SCC was also studied here and it was determined that under present test conditions that is below frequency of 10Hz and ΔK of $\pm 2ksi\sqrt{in}$, SCC had more pronounced effect on the crack growth rate and there was no noticeable difference in crack growth rate for static and fatigue SCC tests at constant K or K_{mean}. More tests shall be conducted with a higher ΔK, $\pm 4ksi\sqrt{in}$.

More investigation on the effect of coatings will be done, also. Machined samples with coatings completely removed have been sent to the OEM to be coated with new coatings, different results may be evident in crack growth rates.

II. References

1. SMN 366, Rev. B, page 8.37. Lockheed-Martin Aeronautics. 1977.
2. Hertzberg, Richard W. Deformation and Fracture Mechanics of Engineering Materials, 4th Edition. John Wiley & Sons, Inc, page 497. ©1996.
3. Speidel, Marcus O. "Stress Corrosion Cracking of Aluminum Alloys." Metallurgical Transactions A. Volume 6A. April 1975-631
4. ASTM E 647 Standard Test Method for Measurement of Fatigue Crack Growth Rates. ASTM International, West Conshohocken, PA.